Positron-annihilation study of the aging kinetics of AlCu-based alloys. I. Al-Cu-Mg

A. Somoza
IFIMAT-UNCentro and Comisión de Investigaciones Científicas de la Provincia de Buenos Aires, Pinto 399, 7000 Tandil, Argentina

A. Dupasquier
Instituto Nazionale di Fisica della Materia and Dipartimento di Fisica, Politecnico di Milano, Piazza Leonardo da Vinci 32, 20133 Milano, Italy

I. J. Polmear
Monash University, Department of Materials Engineering, Clayton, Victoria 3168, Australia

P. Folegati
Instituto Nazionale di Fisica della Materia and Dipartimento di Fisica, Politecnico di Milano, Piazza Leonardo da Vinci 32, 20133 Milano, Italy

R. Ferragut
IFIMAT-UNCentro and Comisión de Investigaciones Científicas de la Provincia de Buenos Aires, Pinto 399, 7000 Tandil, Argentina

(Received 31 August 1999; revised manuscript received 15 December 1999)

Positron-annihilation spectroscopy has been applied for studying the aging kinetics and the association of vacancies to solute elements during precipitation in an Al-Cu-Mg alloy with high Cu/Mg ratio. The results show that: (i) isolated vacancies–Mg complexes exist in the alloy following quenching from the solution treatment temperature; (ii) after aging at temperatures below 68 °C, the vacancies are associated with Cu and with Cu-Mg aggregates [solute clusters, Guinier-Preston GP(Cu) and GP(Cu, Mg) zones]; (iii) the contribution of Cu-Mg aggregates decreases as the aging temperature is raised from 20 to 68 °C; (iv) immediately after aging at 180 °C for times from 15 s to 10 h, the vacancies are present only in pure Cu regions, but vacancies in Cu-Mg aggregates become observable when the sample is cooled and aged at room temperature. The kinetics of formation of solute aggregates can be described, after scaling, by a temperature-independent function. From the temperature dependence of the scaling factors, an effective activation energy of 0.65 eV was obtained.

I. INTRODUCTION

Alloy systems in which the solid solubility of one or more of the alloying elements decreases with decreasing temperature may be amenable to the phenomenon of age hardening.[1] Such a response may be obtained if the alloy is solution treated by holding at relatively high temperature to dissolve the alloying elements and quenching, usually to room temperature, to obtain a supersaturated solid solution (SSSS). The alloy is then hardened by controlled decomposition of the SSSS to form finely dispersed precipitates by holding for convenient times (aging) at one, or sometimes, two, intermediate temperatures. Because of the technological importance of age hardening as a means of strengthening many alloys, precipitation processes continue to stimulate the converging interest of metallurgists, chemists, and solid-state physicists.

The phenomenon of age hardening was discovered in an Al-Cu-Mg alloy by Alfred Wilm in Berlin.[2] This work led to the development of the well-known wrought alloy duralumin which was quickly adopted in Germany for structural members of Zeppelin airships and for the Junkers passenger aircraft that first flew in 1919. Since then many other age hardenable aluminum alloys have been developed. Some will age if held at room temperature after quenching (natural aging) but most are aged at elevated temperatures (artificial aging).

Al-Cu-Mg alloys have remained one of the two major classes of high strength aluminum alloys used for aircraft worldwide. Many ternary Al-Cu-Mg alloys harden in two distinct stages when aged over a wide temperature range (e.g., 100 to 240 °C). The first stage, which may occur very rapidly and accounts for as much as 70% of the total hardening,[3,4] has generally been attributed to the formation of Guinier-Preston zones comprised of Cu and Mg atoms (often known as GPB zones), although their structure and chemistry remain poorly defined.[5–7] More recently, studies by atom probe field ion microscopy (APFIM) and high-resolution electron microscopy have suggested that this first stage of hardening may in fact have its origin in solute clustering rather than in the presence of GPB.[8] The phenomenon has been termed *cluster hardening*.[9,10] What remains uncertain is the role of quenched-in vacancies facilitating nucleation of clusters, zones, and precipitates during the early stage of aging.

The present paper is concerned with the alloy Al-4% Cu-0.3%Mg (wt %) having a high Cu/Mg ratio (~5:1, compositions in at. %) which lies in the $\alpha+\theta$ (Al_2Cu)

 ©2000 The American Physical Society

$+S$ (Al_2CuMg) region of the ternary phase diagram close to the border with the $\alpha+\theta$ region.[11] Then, in a second paper, to be found in the same issue of this journal (referred to below as paper II), a study is made of the effect of microalloying addition of Ag since this element is known to stimulate profound changes in the precipitation process in the ternary alloy.[12,13] Since then, much more detailed information on precipitation processes in these two alloys has come from imaging and diffraction techniques, namely high-resolution transmission electron microscopy, electron diffraction, atom probe field ion microscopy, and the three-dimensional atom probe.[8–10,14–19] This work has provided a detailed background for the present study, which has the following aims:
(i) to investigate directly the role of vacancies in these precipitation processes (which is not possible by any of the above techniques);
(ii) to provide information regarding the aging kinetics of the alloys at constant temperature;
(iii) to establish a methodology that can be used for studies of other age hardenable systems.

The technique adopted for the present work is positron annihilation spectroscopy (PAS), which is specific for the detection of vacancylike defects, and also has a good sensitivity for the chemical environment of this species of lattice defects (for general information of PAS, see Ref. 20; for applications of PAS to the study of aluminum alloy decomposition, see Refs. 21–23). PAS has no sensitivity to crystallography and a very limited sensitivity to geometry. However, in comparison to imaging and diffraction techniques, it has the advantage of being nondestructive, which is an essential quality for *in situ* experiments regarding kinetics. Also, a conventional PAS experiment probes a macroscopic volume of the sample, thus avoiding problems related to poor statistics.

The application of PAS to the study of the decomposition kinetics of alloys at constant temperature has been previously made in a few occasions (see references in Ref. 23), but we believe that this is the first work showing in full the potential of the method. This goal is reached by increasing the counting rate to the extent permitted by commercial equipment for time spectrometry of the annihilation radiation, thereby attaining a rate of data collection sufficient to follow *in situ* transient phenomena (see Sec. II). Our results are presented in Sec. III, with a preliminary discussion based on direct evidences. However, the potential of PAS technique cannot be fully exploited without a quantitative analysis of the results on the basis of a model. This part is discussed in Sec. IV, where we also report, as a result of the analysis, quantitative information on the relative concentration of solute-vacancy aggregates of different composition. Our conclusions are briefly summarized in Sec. IV.

II. SAMPLES AND EXPERIMENTAL TECHNIQUES

The material used in the present work was a laboratory alloy, prepared from high-purity elements. As mentioned above, the nominal composition was Al-4%Cu-0.3%Mg (wt %), equivalent to Al-1.74%Cu-0.35%Mg (at. %). With this composition, the equilibrium microstructure, which can be reached only after long-term aging at relatively high temperatures, is a dispersion of the incoherent precipitates θ (Al_2Cu) and S (Al_2CuMg) in the α-phase matrix (saturated solid solution of Cu and Mg in Al). Aging at lower temperatures may lead to precipitation of the earlier metastable GP(Cu) and GP(Cu, Mg) zones and semicoherent $\theta'+S'$ phases.

The material was melted in a graphite crucible, degassed with chlorine and chill cast into an iron mold $240\times110\times20\,mm^3$. After homogenizing 24 h at 500 °C and scalping, the alloy was rolled to a thickness of 6 mm. Samples for PAS measurements were two small slabs ($10\times10\times0.8\,mm^3$), obtained from a block by spark cutting followed by mechanical polishing. The same pair of samples was used for all the experiments described below. The thermal treatment at the beginning of each experiment was a solution treatment at 520 °C for 25 min in an argon atmosphere, followed by quenching in a cooling bath (normally, an ice-water mixture at 0 °C, with exceptions in the case of experiment 1, as described below). Immediately after quenching, the samples were mounted for PAS measurements and aged at temperatures in the range 20–68 °C (experiments 1–3), or artificially aged at 180 °C in a silicone oil bath for different times from 15 s to 10 h (experiment 4), quenched again and mounted for PAS measurements. The whole process of extracting the samples from the quenching bath, rinsing, drying, mounting as a sandwich with the positron source, and setting in place near to the detectors of the positron lifetime spectrometer was concluded in less than 30 s. During the measurements, the temperature of the samples was kept at 20 °C (experiments 1 and 4) or at a different level (experiments 2 and 3) with the help of a miniaturized electric heater.

The PAS technique adopted in this work was the measurement of the positron lifetime spectrum; this is a standard method for investigations on defects (see, for instance, Ref. 24), based on the property of the positrons to be trapped in certain species of defects. The lifetime spectrum contains a number of components corresponding to the number of different positron states. Analysis of the spectrum gives information on the concentration and on the structure of the traps. The equipment used in the present work was a conventional Ortec fast time spectrometer, equipped with one 1.5 in. $\times$20 mm cylindrical Pilot U plastic, for the start photons (1.28 MeV), and one cylindrical BaF_2 scintillator (1 in. diameter by 10 mm thick), for the stop pulses (0.511 MeV), both coupled to XP2020 Philips photomultipliers without and with quartz window, respectively. For increasing the collection efficiency, the sample was directly sandwiched between the two scintillators. The energy selection was set to accept all pulses in a window extended from 0.80 to 1.36 MeV (start channel) and from 0.41 to 0.55 MeV (stop channel). The positron source (^{22}Na) had an intensity of $\approx1\times10^6$ Bq; the same source, sealed in 7.5-μm Kapton foils, was used for all the measurements. The counting rate was of about 200 coincidences per second, and the time resolution was 250 ps (full width at half maximum). During a measurement run, a lifetime spectrum was collected every 30 min. Some runs were extended up to 1.7×10^6 s of natural aging at 20 °C. The long-term stability of the system was excellent: irregular oscillations of the average positron lifetime, which are barely visible in several of the figures reported below, have an amplitude of less than 0.3 ps in a period of a few hours, and average to nearly zero in periods longer than a

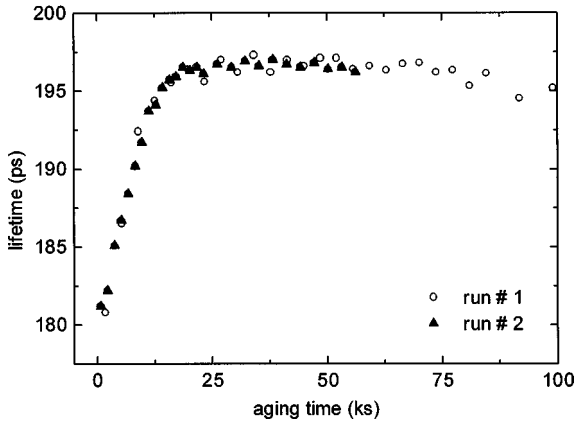

FIG. 1. An example of the reproducibility of the measurements: the two sets of data were taken at the distance of two weeks, after renewing the thermal treatment (solution treatment+quenching at 0 °C+30 s heating at 180 °C+aging at 20 °C). The estimated error bar of each point is 0.5 ps.

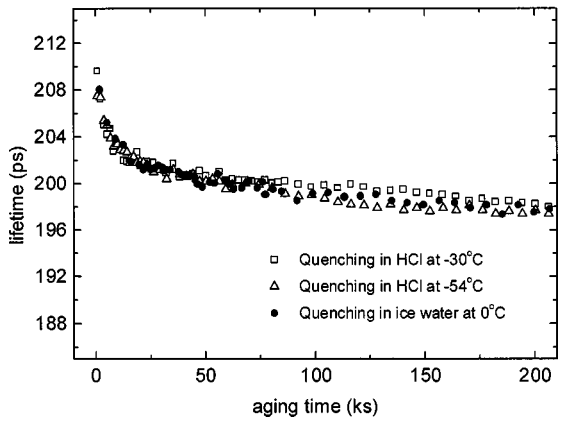

FIG. 2. A test of the effect of changing the quenching procedures: the three sets of data represent the evolution of the positron lifetime during natural aging, after solution treatment, and quenching by immersion in a bath at various temperatures.

few days. An example of the reproducibility of the measurements is given in Fig. 1, which shows the results of two independent runs, taken at the distance of a few weeks. The data regard the evolution that takes place at room temperature after artificial annealing at 180 °C for 30 s.

Some distortion of the time spectrum, including a possible spurious contribution due to gamma rays backscattered from a scintillator to the opposite one, is inevitable with an experimental setup optimized for high counting rate. This distortion was estimated to affect the measured average positron lifetime by a systematic reduction of about 2 ps. The results presented in the present paper are not corrected for this small bias, which is irrelevant for the observation of effects related to the structural evolution of the alloy.

The parameter used for characterizing the interaction of the positron with the material is the average lifetime τ, which was obtained from a Positronfit analysis of the lifetime spectrum after the subtraction of the source component.[25] A single exponential component was always adequate for obtaining a satisfactory fit. Physically, this result might indicate 100% positron trapping in the same type of defect; most probably, however, it is the outcome of competitive trapping in different families of defects, giving lifetimes too close to be isolated with a statistics of less than 0.5×10^6 counts. Single-component spectra have also been observed in Al-Cu-Mg alloys for heat treatments up to ≈250 °C by other groups.[26] In Sec. IV, a model is discussed that implies the presence of two or three components. In order to check the consistency of this model with the Positronfit analysis, fits with constrained lifetimes have also been performed. The obtained intensities were in agreement with the predictions of the model. There was practically no change in the average lifetime. A small improvement in the goodness-of-fit parameter was also observed.

III. RESULTS

A series of experiments were performed to observe the effects of different thermal treatments. Here the outcome of the different experiments is presented separately, with a few comments on the information that can be drawn from it. A more detailed analysis, based on a simplified model, is given in the next section.

A. Experiment 1: Natural aging after different quenching procedures

The common initial step of the different heat treatments given in all the experiments described below is a solution treatment followed by quenching. In principle, unintentional small changes of the cooling rate in repeated experiments could modify the initial content of quenched-in vacancies. In order to ascertain how this element of irreproducibility might affect PAS results, a preliminary experiment was made by measuring the positron lifetime spectra during natural aging at 20 °C after quenching at different temperatures (−54, −30, 0 °C). Results are shown in Fig. 2, where the average positron lifetime is plotted against the aging time. These data indicate that changes in the quenching procedure have little effect, with no apparent correlation being found with the temperature of the quenching bath. Thus it can be excluded that the much bigger effects described below, that were observed by changing the aging treatments, are significantly distorted by unintentional variations of the cooling rate during quenching.

This relative insensitivity of the positron lifetime evolution to the details of the quenching may seem surprising, knowing that the positron lifetime is affected by the presence of vacancies, and that the initial concentration of vacancies is certainly a function of the quenching rate. However, it should be recalled that the measurement giving the first point of any of the curves in Fig. 2 takes 30 min. This time interval is long enough to permit the migration at room temperature of isolated vacancies to surfaces and sinks,[27,28] and the collapse of large vacancy clusters to form dislocation defects Thus PAS data do not reflect the initial concentration of free vacancies, but rather that of less mobile vacancy-solute complexes (both Mg and Cu are known for binding effectively vacancies in Al). After an efficient heat treatment (i.e., negligible solute clustering during the quenching), the concentration of these complexes will be controlled only by the concentration of the solute. This is sufficient to give satura-

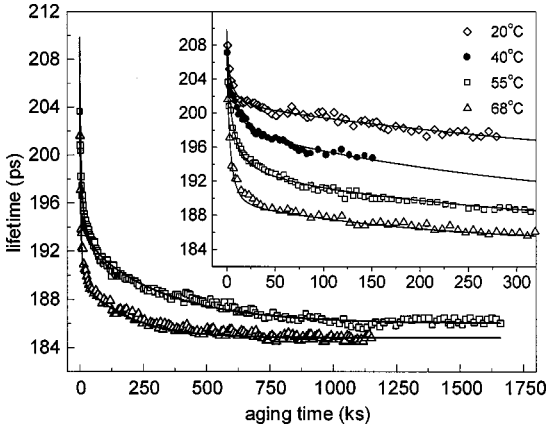

FIG. 3. Positron lifetime evolution at various temperatures, after solution treatment and quenching at 0 °C. The best-fit curves through the experimental points are calculated on the basis of the positron-trapping model.

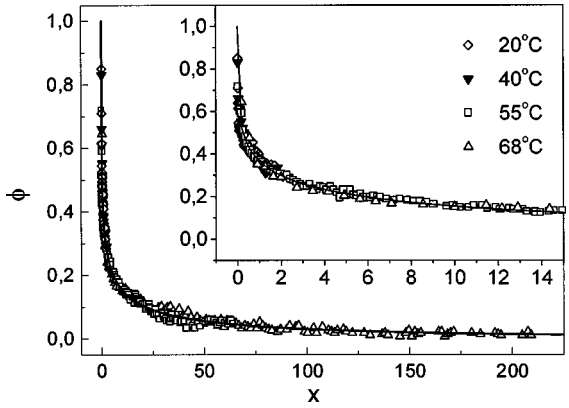

FIG. 4. Degree of freshness $\Phi=(\tau-\tau_\infty)/(\tau_0-\tau_\infty)$ versus scaled aging time $x=t/t^*$. This figure is obtained by scaling the data in Fig. 3 (not all the experimental points are shown). The master curve through the experimental points is the Kohlrausch function with $\beta=0.272$.

tion trapping (i.e., 100% of the positrons are annihilated in a trap). The initial lifetime (the highest measured value is 210 ps, but the extrapolated value at $t=0$ is 212 ps) must therefore be identified with positron trapping at vacancies bound to a single solute atom, or to a small cluster of solute atoms. Most probably, vacancies are attached to single Cu or Mg atoms that contribute to the lifetime spectrum with components giving a lifetime difference too small to be resolved in the present experimental situation. Similar results were obtained by Dlubek *et al.*; [26] they quote a lifetime of 208 ps for the binary alloy Al-2%Cu (at. %) and 212 ps for the ternary system Al-2%Cu-0.26%Mg (at. %).

B. Experiment 2: One-stage aging at 20, 40, 55, and 68 °C

This experiment was designed to study the evolution of the alloy at temperatures low enough to avoid formation of semicoherent or incoherent precipitates. The samples were solution treated and quenched as described above, and isothermally aged at selected temperatures (20, 40, 55, and 68 °C). Measurements of the positron lifetime spectra were performed *in situ* at these temperatures and results are shown in Fig. 3.

All the curves in Fig. 3 display a monotonic decrease of τ, with a rapid initial drop followed by a slower stage. The decrease becomes faster and more pronounced as the aging temperature increases. At the two highest temperatures (55 and 68 °C) a horizontal asymptote becomes visible.

The dependence of the positron lifetime on the aging time is the result of the decreasing probability of positron trapping at isolated vacancy-solute pairs, with a concomitant increase of the probability of trapping at vacancies contained in solute-enriched regions [solute clusters, GP(Cu) and GP(Cu, Mg) zones]. Thus the lifetime data of Fig. 3 give information on the kinetics of the alloy decomposition, which is filtered through the enhanced sensitivity of PAS to the structures that contain vacancies. Remarkably, it can be shown that this kinetics obeys a very simple scaling law. To this end, it is convenient to describe the positron lifetime evolution from the initial value τ_0 toward the asymptote τ_∞ by using the reduced variable

$$\Phi=\frac{\tau-\tau_\infty}{\tau_0-\tau_\infty} \tag{1}$$

which can be considered a measure of the ''degree of freshness'' of the sample. Figure 4 shows the dependency of Φ on a scaled time variable $x=t/t^*$, where the scaling factor t^* is a function of the temperature T of the aging treatment. The values of the parameters τ_0, τ_∞, t^* used for obtaining Fig. 4 depend on T as given in Table I.

A best fit of the scaling factors t^* with the Arrhenius relationship $t^*=A\exp(E_a/k_BT)$, where k_B is the Boltzmann constant and T the absolute temperature, gives the activation energy $E_a=0.65\pm0.05$ eV (a figure showing the Arrhenius plot can be found in Ref. 29).

The master curve running through the data points in Fig. 4 is the Kohlrausch function $\Phi=\exp(-x^\beta)$, with $\beta=0.272\pm0.002$. It should be noted that the Kohlrausch function (with $\beta<1$) describes a complex decay with a spectrum of decay rates.[30,31] For this reason, the activation energy E_a reported above is to be considered as an effective value that determines the kinetics of the decay, but which cannot be related to a specific atomistic process. This subject is further discussed in Ref. 29.

The dependence of the asymptotic value of the positron lifetime on the aging temperature is an important point, since it indicates a change of the chemical environment of the annihilation site, which most probably is a vacancy in a GP zone.[21,22] Thus it gives information regarding the average Mg/Cu concentration ratio near to vacancies in the final con-

TABLE I. Time scaling factor t^* and other parameters used for the calculation of the ''degree of freshness'' Φ [Eq. (1)] at various aging temperatures T.

T (°C)	τ_0 (ps)	τ_∞ (ps)	t^* (ks)
20	212	191	200
40	212	188	60
55	212	185	23
68	212	184.5	5.8

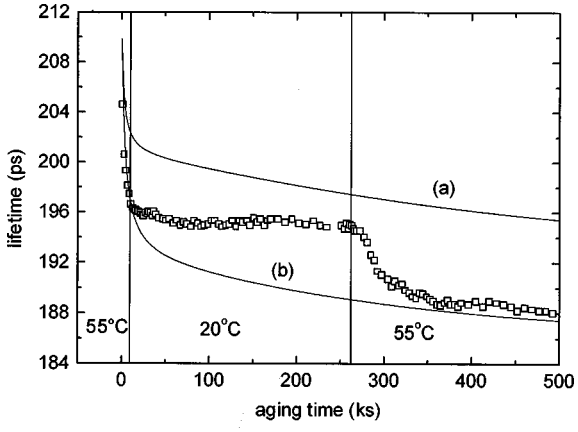

FIG. 5. Evolution of the positron lifetime during aging at 55 °C (up to 10 ks)+aging at 20 °C (up to 263 ks)+aging at 55 °C (from 263 ks). The lines labeled (a) and (b) are the expected decay curves at 20 and at 55 °C, respectively (from Fig. 3).

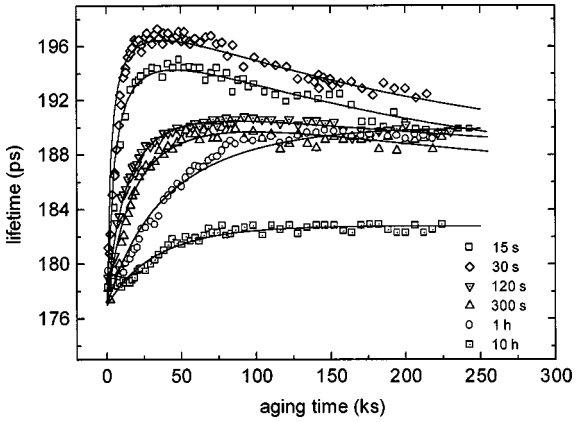

FIG. 6. Evolution of the positron lifetime during natural aging after solution treatment+quenching at 0 °C+heat treatment at 180 °C for various times (as indicated in the figure). The best-fit curves through the experimental points are calculated on the basis of the positron-trapping model.

dition reached after a prolonged aging. An attempt to obtain this information in quantitative terms will be presented below (Sec. IV).

C. Experiment 3: Switching between 55 and 20 °C during aging

In principle, the different final conditions reached at the various aging temperatures that were noted above might have different explanations. One possibility could be that the average composition of the GP zones is reversibly controlled by the solubility of the different alloying elements. In this case, the temperature dependence of the composition of the GP zones would just reflect the different temperature dependence of the solubilities of Cu and Mg. With this kind of mechanism, switching between two temperatures should produce reversible changes of the composition of the GP zones and experiment 3 was devised to check this hypothesis. The data of Fig. 5 show what actually happens when the temperature of aging is repeatedly switched between 20 and 55 °C.

Clearly, these data do not support the hypothesis of reversible changes. An abrupt increase of temperature enables the structures formed at low temperature to evolve toward the high-temperature form (observe a knee in the curve at 263 ks). On the contrary, a decrease of the temperature stops the evolution (observe a knee at 10 ks, followed by a plateau), but does not promote reversion of the high-temperature structures into the low-temperature form. This unidirectional behavior demonstrates that the energetic stability of the structures formed at various temperatures increases with the temperature at which they form. Consequently, the existence of different structures is then to be ascribed to a kinetic effect, i.e., to the temperature dependency of the mobilities of the different solutes.

D. Experiment 4: Artificial aging at 180 °C followed by natural aging at 20 °C

For the alloy studied in the present work, a long aging treatment at 180 °C may lead to the eventual formation of the equilibrium phases θ and S. However, the formation of these and other phases is believed to begin by the formation of solute clusters, which keep evolving in size, structure, and composition.[17] During the growth of the clusters and the possible formation of GP zones, the supersaturation of the matrix decreases gradually. If the aging treatment is interrupted at an early stage, the residual supersaturation may be sufficient to promote further precipitation at room temperature. The aim of the experiment was to observe the conditions of the alloy just after aging at 180 °C and to monitor possible further changes on holding at room temperature.

After solution treatment and quenching, the samples were aged at 180 °C for different times: 15 s, 30 s, 120 s, 300 s, 1 h, and 10 h. At the end of each aging cycle, the samples were quenched to 0 °C, rapidly brought at room temperature (20 °C) and positron lifetime measurements were initiated immediately. Figure 6 shows the results.

A linear extrapolation to $t=0$ of the curves in Fig. 6 (in the interval $t<10$ ks) enables estimation of the average positron lifetime τ_{aa} at the end of each aging cycle at 180 °C. This information is displayed in Fig. 7, as a function of aging time.

Comparing the data of Fig. 7 with the results of experiments 1 and 2 indicates that the effect of the aging treatment on the positron lifetime is extremely strong and very rapid: the lifetime drops from $\tau_0=212$ ps (see Table I) to below

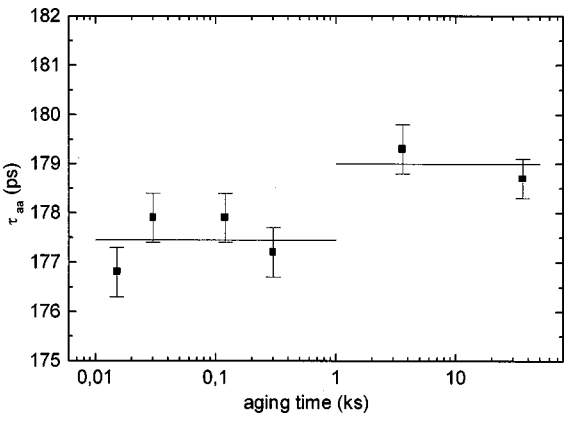

FIG. 7. Positron lifetime immediately after artificial aging at 180 °C, plotted versus the duration of the artificial aging.

177 ps in only 15 s at 180 °C. Lifetime changes of this magnitude are unusual in aging experiments and can be explained only by the rapid formation of a new structure, that acts as a very effective positron trap. Figure 7 also indicates that, within the experimental indetermination, τ_{aa} is constant up to 300 s. This result means that the chemical composition probed by the positron in the new trap does not change (within the sensitivity limits of our technique). A value of about 177 ps for the initial lifetime suggests that the positron trap is a Cu structure (cluster or precipitate) containing vacancies.[32] The small increase of τ_{aa} (about 1.6 ps), which occurs with heat treatments of 1 and 10 h, could be the effect of a change in the average composition of the solute aggregates, but most probably is the signature of the formation of the semicoherent precipitates that appear with the artificial aging at 180 °C.[17] Positrons would be trapped in the misfit region at the interface between the matrix and the precipitates, where their lifetime is slightly increased because of a reduced overlap with Cu atoms.[26]

The conditions observed at the end of the aging treatment are consistent with the results of hardness measurements (the first hardening stage, believed to be an effect of solute clustering, occurs after a few seconds at temperatures above 150 °C), with TEM images of GP(Cu) zones (disc-shaped arrays of Cu atoms on the lattice cube planes) and with direct APFIM observation of Cu clusters.[9,17,18] A point of difference with the results of Ringer and co-workers[9,17,18] is that they also have evidence of Cu and Mg co-clustering and, after 9 ks at 180 °C, precipitation of the S' phase, whereas no effect that can be ascribed to the aggregation of Mg (alone or with Cu) was observed in the present work. According to Reich *et al.*,[19] the possibility that the Cu-Mg co-clustering observed by Ringer *et al.* occurs after the alloy has been aged at 180 °C may be rejected because the manipulation of the samples and the APFIM measurements were performed at a very low temperature (~25 K). Therefore an explanation of the difference must be sought in the accuracy limits of our technique. Including the error bars, the total excursion of τ_{aa} for artificial aging up to 30 s at 180 °C is of the order of 2 ps (see Fig. 7). This uncertainty can hide a contribution of vacancies associated to Cu-Mg aggregates (for which the positron lifetime is expected to be above 200 ps) if the corresponding positron trapping rate is less than 10% of the trapping rate of the dominant population of Cu aggregates. If the average sizes of the two families of clusters are similar, the ratio of the trapping rates is a good indication of the ratio of the number densities. The above estimate (10%) is in reasonable agreement with expectations based on equilibrium data. The Mg content of our samples (0.30 wt %) places the alloy just beyond the border between the $\alpha+\theta$ and $\alpha+\theta+S$ phase regions at 180 °C: a phase diagram at 190 °C (Brook 1963) sets this border at ≈0.25 wt % Mg. Using this datum, one evaluates the ratio of the numbers of Cu-Mg aggregates (precursors of S particles) and of Cu aggregates (precursors of θ particles) at about 8%.

The results shown in Fig. 6 suggest that further aging has occurred at room temperature after the alloys has been exposed for as long as 10 h at 180 °C. This is a surprising result because it may be expected that aging at 180 °C would stabilize the alloy.

The interpretation of the experimental results of PAS in terms of structural modifications of the alloy requires further attention. A variety of behaviors has been observed that cannot be reduced to a common pattern described by a master curve, as in the case of one-stage aging (see above). The curves can be classified in three categories:

(i) curves with a maximum (aging treatments of 15 and 30 s);

(ii) curves with a monotonic increase to a plateau (aging treatments of 120 and 300 s);

(iii) curves with a small initial plateau, followed by a monotonic increase to a second plateau (aging treatments of 1 and 10 h).

Taking as a basic assumption for any interpretation that precipitates formed at 180 °C are more stable than those formed at 20 °C, then it may be assumed that the formed precipitates will not dissolve when the temperature decreases. Thus the present observations demonstrate the formation of some additional clusters or precipitates at room temperature, which act as positron traps in competition with those already existing. The lifetime increase above the initial point (a common feature for the three categories) indicates that at least some of new structures contain vacancies in an Mg-rich environment. The solute needed for forming these new clusters must come from the residual Mg supersaturation (at 20 °C), surviving in the matrix after aging at 180 °C. A somewhat different situation occurs with Cu. There is immediate evidence of new Cu structures formed at 20 °C only for short aging treatments (15 and 30 s), given by the nonmonotonic behavior of the positron lifetime curves. Indeed, the condition for the existence of a maximum in the lifetime curve is that pure Cu structures, responsible for a shortening of the lifetime, are formed at 20 °C with a slower time law than the structures containing Mg, which give a positron lifetime longer than pure Cu aggregates. On the contrary, the present results do not give an immediate indication of Cu supersaturation surviving after aging treatments of 120 s or longer at 180 °C. This point will be discussed further in the next section, on the basis of a quantitative analysis.

IV. MODEL ANALYSIS

So far, care has been taken to present only empirical evidence, in order to avoid any possible contamination of facts with theories. This approach allows a simple mathematical description to be given of the kinetics at moderate temperatures, and to evaluate the corresponding characteristic parameters. However, it may be interesting to gain a deeper insight of the interplay of factors that determine the impressive variety of behaviors depicted in Figs. 4 and 6. In the present section, it is shown that all these results can be framed in a comprehensive picture, from which quantitative information regarding the structure of the alloy and its transformation kinetics can be derived. To this end, the widely accepted positron-trapping model can be used as a guideline for a mathematical interpretation. Unfortunately, the real situation that occurs in an alloy containing solute clusters of variable chemical composition implies an extended spectrum of positron states, which cannot be accounted in full by trapping model analysis without introducing too many arbitrary parameters. However, even a simplified model that assumes only three different species of positron traps is sufficient for

TABLE II. Results of the model analysis for experiment 2.

T (°C)	K_1^0/K_3^∞	K_2^∞/K_3^∞	t_1 (ks)	t_2 (ks)	t_3 (ks)	χ^2
20	$(51\pm2)\times10^{-3}$	1.49 ± 0.01	100 ± 20	83 ± 10	539[a]	0.52
40	$(43\pm2)\times10^{-3}$	0.73 ± 0.01	61 ± 10	87 ± 10	440 ± 20	0.64
55	$(25\pm1)\times10^{-3}$	0.533 ± 0.005	50 ± 10	100 ± 10	310 ± 10	0.65
68	$(20\pm1)\times10^{-3}$	0.405 ± 0.005	13 ± 2	87 ± 4	212 ± 6	0.64

[a]Value fixed for all room-temperature measurements.

reproducing the monotonic decay observed in experiment 2, as well as the monotonic and nonmonotonic curves observed in experiment 4. The morphology of the different species of traps cannot be uniquely defined, because each species of the model actually represents a family of similar, although not identical, traps existing in the alloy (for instance, vacancies decorated with a different number and species of solute atoms). A possible characterization of the three families of traps is as follows:

(i) trap 1: vacancies decorated with a single solute atom (Mg or Cu); associated positron lifetime $\tau_1=212$ ps;

(ii) trap 2: vacancies in a mixed Cu/Mg-rich environment (Cu/Mg co-clusters, GPB zones); associated positron lifetime $\tau_2=203$ ps;

(iii) trap 3: vacancies in a Cu-rich environment (Cu clusters, GP zones); associated positron lifetime $\tau_3=177$ ps.

The above values of the lifetimes, which were heuristically assigned on the basis of the experimental curves, are in reasonable agreement with published data.[26,32] The presence of isolated vacancies was not taken in consideration not only because a characteristic positron lifetime above 240 ps (Refs. 33 and 34) was not observed, but also because it is well known that single vacancies in Al migrate in a few minutes at temperatures below 0 °C.[27,28]

In conditions of saturated trapping the average positron lifetime, which is the experimental parameter used in the present work, is $\tau=\Sigma_{i=1,3}w_i\tau_i$, where the w_i's are the intensities of the lifetime components associated to the three species of trap and the τ_i's are the lifetimes. The normalization condition is $\Sigma_{i=1,3}w_i=1$. According to the trapping model, the w_i's can be expressed in terms of the trapping rates k_i as given by the equation

$$w_i=\frac{k_i}{\tau_{\text{bulk}}^{-1}-\tau_i^{-1}+\sum_{j=1,3}k_j}\approx\frac{k_i}{\sum_{j=1,3}k_j}, \tag{2}$$

where the final approximate result implies saturated trapping. The positron trapping rates are the parameters that must be known in order to interpret possible cluster formation in the alloy, since they are expected to be proportional to the number density of the traps (the coefficient of proportionality may depend, however, on the size and the composition of the trap). In order to reproduce the observed kinetics, it is assumed that the k's evolve monotonically during the aging as described below:

(i) Trap 1 is unstable at room temperature; it is present after the quenching from the solution treatment temperature, but progressively disappears during the aging. This behavior is described by assuming the decay law

$$k_1=K_1^0\exp(-t/t_1); \tag{3}$$

(ii) Traps 2 and 3 are structures formed after quenching; their concentration increases during aging at room temperature. The corresponding trapping rates also increase, with a time law assumed to have the form

$$k_2=K_2^0+(K_2^\infty-K_2^0)[1-\exp(-t/t_2)], \tag{4}$$

$$k_3=K_3^0+(K_3^\infty-K_3^0)[1-\exp(-t/t_3)]. \tag{5}$$

In the above equations, K_i^0 is the value of the trapping rate at the beginning of room temperature aging, K_i^∞ is the asymptotic limit of the trapping rate at $t\to\infty$, and t_i are characteristic time constants. One of the K's parameters can be assigned arbitrarily, because in conditions of saturation trapping, the average lifetime depends on the ratios between the trapping rates but not on their absolute values. Considering the different experimental situations, as explained below, can further reduce the number of unknown parameters.

A. Analysis of experiment 2

In the case of one-stage aging, the lifetime value of 212 ps extrapolated at $t=0$ (with the Kohlrausch function) indicates that trap 1 is the dominant species immediately after the solution treatment, while the solute clusters containing trap 2 and trap 3 are not yet formed ($K_2^0=K_3^0=0$). The ratio K_2^∞/K_3^∞ can be fixed in accordance with the asymptotic lifetimes τ_∞ reported in Table I, using the relationship $K_2^\infty/K_3^\infty=(\tau_3-\tau_\infty)/(\tau_2-\tau_\infty)$. However, this constraint was imposed in preliminary fittings, and then was removed for a fine adjustment. Other best-fit parameters are the ratio K_1^0/K_3^∞ and the characteristic times t_i. No constraint was imposed on the t_i's. To assume the validity of a scaling rule in accordance with the t^* data in Table I would imply a hypothesis on the kinetics of the three families of traps that we are unable to justify on the basis of physical arguments. However, in the case of the curve taken at 20 °C, t_3 was fixed at the same value used for the fitting of the curves taken at 20 °C after a heat treatment at 180 °C (see below). The results are given in Table II. The goodness-of-fit parameter reported in the table is defined by the relationship

$$\chi^2=\frac{\text{variance not explained by the model}}{\text{average variance of the experimental points}}.$$

The denominator of the above fraction is $\sigma^2=(0.5\text{ ps})^2$.

The data reported in Table II give the following indications:

(i) The initial drop of the lifetime curves of Fig. 3 is associated to the migration of small vacancy-solute complexes

(trap 1), with a concomitant increase of trapping at vacancies contained in Cu/Mg co-clusters or in GPB zones (trap 2). The characteristic time t_1 is clearly a decreasing function of the temperature, as expected for a thermally activated process. A weaker temperature dependency of the characteristic time t_2, if it exists, is obscured by the experimental indetermination.

(ii) The slower decrease occurring at long times is associated to additional trapping in vacancies contained in Cu clusters (or GP zones). The characteristic time t_3 decreases with increasing temperature.

(iii) The trapping rate K_1^0 cannot depend on the temperature of aging, since it represents the initial condition before any aging. Thus, the decrease with T of the ratio K_1^0/K_3^∞ indicates that the formation of Cu-rich aggregates is favored by a temperature increase. The present results are in fair quantitative agreement with the preliminary data of a coincidence Doppler broadening experiment (CoPAS) on alloy Al-4.38% Cu-1.67% Mg (wt %) by Biasini,[35] who has observed that, after 1 week aging at 60 °C, the characteristic Cu peak at $\approx 16 \times 10^{-3}$ mc is more intense by a factor ≈ 2 than after 1 week aging at 20 °C.

(iv) The ratio K_2^∞/K_1^0 (as obtained by dividing the data of the third column of Table II by those of the second column) has an average value of 22, with a standard deviation of 5. These data do not indicate any temperature enhancement of the final content of Cu/Mg aggregates. This result can be explained if the aggregation of Mg is complete at all the temperatures of our experiment.

(v) In accordance with points (iii) and (iv), the decrease of the asymptotic lifetime with the temperature finds an explanation in the different concentration ratio of vacancies contained in Cu-Mg zones relative to vacancies in pure Cu zones. The temperature dependency of ratio K_2^∞/K_3^∞ gives a quantitative characterization of the phenomenon. It is remarkable that this ratio always remains well above to the Mg/Cu atomic concentration ratio (20%). This effect suggests either an incomplete Cu aggregation, even after prolonged exposure at temperatures up to 68 °C, or the formation of small Cu aggregates with no vacancies.

B. Analysis of experiment 4

In the case of room temperature aging after aging at 180 °C, the data shown in Fig. 6 suggest that at $t=0$ (beginning of the room-temperature aging) the positrons are predominantly trapped at vacancies contained in Cu-rich aggregates. The contributions of isolated vacancy-solute pairs and Mg/Cu aggregates seem completely negligible ($K_1^0=K_2^0=0$). The choice $K_1^0=K_2^0=0$ does not allow for a small initial plateau visible in the experimental curves corresponding to $\Delta t_{180\,^\circ C}=1$ and 10 h. The present simplified model cannot account for this detail, which is probably due to positron trapping in the misfit region around semicoherent precipitates formed after sufficiently long heat treatments. Thus, for these two curves, the few points on the initial plateau were not included in the fitting. The best-fit parameters were the characteristic times t_2 and t_3, as well as the ratios K_2^∞/K_3^∞ and K_3^0/K_3^∞. The ratio K_2^∞/K_3^∞ was fixed when it could be clearly determined from a horizontal asymptote of the experimental curves using the relationship $K_2^\infty/K_3^\infty=(\tau_3-\tau_\infty)/(\tau_2-\tau_\infty)$. A preliminary fitting run gave t_3 values averaging at 539 ks, with a standard error of 8.7 ks and in the final fitting a value of $t_3=539$ ks has been fixed. As shown in Table II, we obtain an excellent fit with this value of t_3 even for the data of experiment 2 (one-stage natural aging). The other results of the fitting are reported in Table III.

TABLE III. Results of the model analysis for experiment 4.

$\Delta t_{180\,^\circ C}$	K_2^∞/K_3^∞	K_3^0/K_3^∞	t_2 (ks)	χ^2
15 s	0.41 ± 0.02	$(8.2\pm0.5)\times10^{-2}$	32 ± 2	0.90
30 s	0.50 ± 0.02	$(5.4\pm0.5)\times10^{-2}$	32 ± 2	1.27
120 s	0.41 ± 0.02	$(8.1\pm0.5)\times10^{-2}$	96 ± 3	0.65
300 s	0.40 ± 0.02	$(23\pm1)\times10^{-2}$	50 ± 4	0.80
1 h	0.73 ± 0.02	$(71\pm2)\times10^{-2}$	90 ± 4	1.36
10 h	0.27 ± 0.03	$(96\pm2)\times10^{-2}$	41 ± 2	0.44

These data give the following information:

(i) The successful fitting obtained with the present model (see Figs. 4 and 6 for a visual appraisal of the quality of the fits) is the demonstration that even the nonmonotonic behaviors, observed after short heat treatments, can be the result of monotonic changes in the concentration of different positron traps.

(ii) The ratio K_3^0/K_3^∞ (initial trapping rate in Cu aggregates divided by the asymptotic value of the same trapping rate) increases with $\Delta t_{180\,^\circ C}$ for $\Delta t_{180\,^\circ C}\geqslant 30$ s. This effect is clearly the response to the increasing importance of Cu clustering during the heat treatment. After 10 h at 180 °C, almost no Cu is left for producing more clusters at 20 °C.

(iii) The minimum of K_3^0/K_3^∞ at $\Delta t_{180\,^\circ C}=30$ s is not an artifact of the fitting. It corresponds to a remarkable inversion of the relative position of the curves (Fig. 6 shows that the curve for 30 s is higher than those for 15 and for 120 s). The reproducibility of this surprising effect has been checked (see Fig. 1). A tentative explanation could be a reversion phenomenon regarding small Cu clusters formed during the quench.

(iv) The ratio K_2^∞/K_3^∞ (asymptotic value of the trapping rate at defects associated to Mg/Cu aggregates divided by the asymptotic value of the trapping rate at defects in Cu-rich environments) has small variations, probably accidental, for $\Delta t_{180\,^\circ C}\leqslant 300$ s. On the contrary, marked variations in opposite directions occur with heat treatments of 1 and 10 h. The effect must be related to a specific change in the morphology of the aggregates.

V. CONCLUSIONS

The quantitative analysis of our results has been made at two levels. A strictly empirical approach, with no assumptions regarding any microscopic mechanism, shows that an accurate description of one-stage aging (at temperatures not higher than 68 °C) is possible in terms of a scaling law that takes the form of a Kohlrausch function. The kinetics of the process is quantitatively characterized by means of an apparent activation energy of 0.65 eV.

The second level of analysis, based on a simplified version of the positron-trapping model, suggests the following conclusions:

(i) Free vacancies [positron lifetime signal expected at about 240 ps (Refs. 33 and 34)] disappear too quickly to be observed by the technique adopted in the present work. On the contrary, vacancies decorated by a single solute atom (positron lifetime signal at 212 ps) are observed. The concentration of solute-vacancy pairs decays at room temperature with a characteristic time of the order of one day after quenching. The decay is faster at higher temperature (a few hours at 68 °C).
(ii) The signal of vacancy-solute pairs disappears when more effective positron traps are formed. These traps are various types of solute aggregates, containing vacancies.[21,22] Positrons impinging on solute aggregates are trapped very efficiently. The data in Table II show that the positron trapping rates at solute clusters are approximately two orders of magnitude bigger than the trapping rates at vacancy-solute pairs, even if the number density of isolated vacancy-solute pairs that survive after quenching is certainly bigger than that of the clusters.
(iii) Vacancies associated to Cu/Mg aggregates [co-clusters or GP(Cu, Mg) zones] are absent (or below sensitivity) after the solution treatment, quenching and artificial aging at 180 °C. Their concentration increases during aging at moderate temperature with characteristic times of the order of a day.
(iv) Vacancies associated to pure Cu aggregates [clusters or GP(Cu) zones] are absent after the solution treatment and quenching. Their concentration increases during aging with characteristic times of the order of a week at room temperature.
(v) The formation of pure Cu aggregates with vacancies is strongly accelerated by aging at higher temperature. After only 15 s at 180 °C, pure Cu clusters are already clearly observable. A reversion phenomenon, leading to the dissolution of the smallest Cu clusters, is suspected to occur within about 30 s, but after this initial period the growth of Cu aggregates at 180 °C is stable. After 1 h at 180 °C there is a possible signal of the formation of misfit surfaces due to the nucleation of a new phase such as θ'.
(vi) Although the presence of the *S* phase after an artificial aging of 9 ks at 180 °C is confirmed by TEM,[9] a corresponding signal in the positron lifetime spectrum (expected at 240 ps, according to Dlubek *et al.*[26]) was not observed.

Special mention should be made of observation that aging continues to occur at 20 °C following earlier exposure at the relatively high temperature of 180 °C. Additional aging has been previously observed when more highly saturated alloys, such as 2090 [Al-2.7% Cu-2.2% Li (at. %)], are exposed for prolonged times at slightly elevated temperatures (60 to 135 °C),[36,37] following earlier aging at a higher temperature (e.g., 190 °C). However, this effect has not been reported following subsequent exposure at room temperature.

Our final comment concerns methodological aspects. The experimental procedure adopted in the present work can be applied for future studies regarding other alloys. The only instrumental requirement is a setting of the lifetime spectrometer for maximum counting efficiency. The model used for obtaining quantitative data on the relative trapping rates is very simple from both the physical and mathematical points of view. The correct application of the model depends, of course, on the correct assignment of the fixed numerical parameters: here some experience and, most important, tabulations of positron lifetimes in different structures (as, for instance, in Ref. 26) are certainly useful.

ACKNOWLEDGMENTS

This work was partially supported by the Consejo Nacional de Investigaciones Científicas y Técnicas (PIP/BID No. 4318/97), Agencia Nacional de Promoción Científica y Tecnológica (PICT No. 0192/97), Comisión de Investigaciones Científicas de la Provincia de Buenos Aires, and Secretaría de Ciencia y Técnica (UNCentro), Argentina.

[1] L. F. Mondolfo, *Aluminium Alloys: Structure and Properties* (Butterworth, London, 1976).
[2] A. Wilm, Metallurgie (Halle) **8**, 22 (1911).
[3] H. K. Hardy, J. Inst. Met. **83**, 17 (1954–55).
[4] J. T. Vietz and I. J. Polmear, J. Inst. Met. **94**, 410 (1966).
[5] H. Lambot, Bull. Cl. Sci., Acad. R. Belg. **26**, 1609 (1950).
[6] Yu. A. Bagaryatsky, Dokl. Akad. Nauk (SSSR) **87**, 559 (1952).
[7] J. M. Silcock, J. Inst. Met. **89**, 203 (1960–61).
[8] K. Hono, Acta Mater. **47**, 3127 (1999).
[9] S. P. Ringer, K. Hono, I. J. Polmear, and T. Sakurai, Acta Mater. **44**, 1883 (1996).
[10] S. P. Ringer, K. Hono, I. J. Polmear, and T. Sakurai, Appl. Surf. Sci. **94/95**, 253 (1996).
[11] G. B. Brook, Special Report No. 3, Fulmer Research Institute, UK, 1963 (unpublished).
[12] R. J. Chester and I. J. Polmear, *The Metallurgy of Light Alloys* (The Institution of Metallurgists, London, 1983), p. 75.
[13] J. A. Taylor, B. A. Parker, and I. J. Polmear, Met. Sci. **12**, 478 (1978).
[14] K. M. Knowles and W. M. Stobbs, Acta Crystallogr., Sect. B: Struct. Sci. **44**, 207 (1988).
[15] B. C. Muddle and I. J. Polmear, Acta Metall. **37**, 777 (1989).
[16] K. Hono, T. Sakurai, and I. J. Polmear, Scr. Metall. Mater. **30**, 695 (1994).
[17] S. P. Ringer, T. Sakurai, and I. J. Polmear, Acta Mater. **45**, 3731 (1997).
[18] S. P. Ringer, G. C. Quan, and T. Sakurai, Mater. Sci. Eng., A **250**, 120 (1998).
[19] L. Reich, M. Murayama, and K. Hono, Acta Mater. **46**, 6053 (1998).
[20] *Positron Spectroscopy of Solids*, edited by A. Dupasquier and A. P. Mills, Jr. (IOS, Amsterdam, 1995).
[21] G. Dlubek, Mater. Sci. Forum **13/14**, 15 (1987).
[22] R. Krause, G. Dlubek and O. Brümmer, in *Proceedings of the European Meeting on Positron Studies of Defects*, edited by G. Dlubek, O. Brümmer, and K. Henning (Martin Luther University, Halle, Germany, 1987), Plenary Lecture 7.
[23] A. Dupasquier, P. Folegati, N. de Diego, and A. Somoza, J. Phys.: Condens. Matter **10**, 10 409 (1998).
[24] P. Hautojärvi and C. Corbel, in *Positron Spectroscopy of Solids*, edited by A. Dupasquier and A. P. Mills, Jr. (IOS, Amsterdam, 1995), p. 491.

[25] P. Kirkegaard, N. J. Petersen, and M. Eldrup, PATFIT-88 Program, Risø National Laboratory, M-2740 (Roskilde, Denmark, 1989).
[26] G. Dlubek, P. Lademann, H. Krause, S. Krause, and R. Unger, Scr. Mater. **39**, 893 (1998).
[27] T. Federighi, S. Ceresara, and F. Pieragostini, Philos. Mag. **12**, 1093 (1965).
[28] S. Mantl and W. Triftshäuser, Phys. Rev. B **17**, 1645 (1978).
[29] A. Somoza, A. Dupasquier, I. J. Polmear, P. Folegati, and R. Ferragut, following paper, Phys. Rev. B **61**, 14 464 (2000).
[30] R. Kohlrausch, Poggendorff's Ann. Phys. **1**, 179 (1854).
[31] J. Jäckle, Rep. Prog. Phys. **49**, 171 (1986).
[32] H.-E. Schaefer, W. Stuck, F. Banhart, and W. Bauer, Mater. Sci. Forum **15-18**, 117 (1987).
[33] M. J. Fluss, L. C. Smedskjaer, M. K. Chason, D. G. Legnini, and R. W. Siegel, Phys. Rev. B **17**, 3444 (1978).
[34] H.-E. Schaefer, R. Gugelmaier, M. Schmoltz, and A. Seeger, Mater. Sci. Forum **15-18**, 111 (1987).
[35] M. Biasini (private communication).
[36] E. S. Balmuth and D. J. Chellman, in *Proceedings of the 4th International Conference on Aluminium Alloys*, edited by T. H. Sanders and E. A. Starke, Jr. (Georgia Institute of Technology, Atlanta, 1994), Vol. 2, p. 72.
[37] M. J. Kerr, E. D. Sweet, C. G. Bennett, and B. C. Muddle, Mater. Sci. Forum **217-222**, 1079 (1996).